Antivitamins

International Edition: DOI: 10.1002/anie.201701583
German Edition: DOI: 10.1002/ange.201701583

Antivitamin B_{12} Inhibition of the Human B_{12}-Processing Enzyme CblC: Crystal Structure of an Inactive Ternary Complex with Glutathione as the Cosubstrate

Markus Ruetz, Aranganathan Shanmuganathan, Carmen Gherasim, Agnes Karasik, Robert Salchner, Christoph Kieninger, Klaus Wurst, Ruma Banerjee, Markos Koutmos,* and Bernhard Kräutler**

Dedicated to Professor Ebba Nexø

Abstract: *B_{12} antivitamins are important and robust tools for investigating the biological roles of vitamin B_{12}. Here, the potential antivitamin B_{12} 2,4-difluorophenylethynylcobalamin (F2PhEtyCbl) was prepared, and its 3D structure was studied in solution and in the crystal. Chemically inert F2PhEtyCbl resisted thermolysis of its Co–C bond at 100 °C, was stable in bright daylight, and also remained intact upon prolonged storage in aqueous solution at room temperature. It binds to the human B_{12}-processing enzyme CblC with high affinity (K_D = 130 nM) in the presence of the cosubstrate glutathione (GSH). F2PhEtyCbl withstood tailoring by CblC, and it also stabilized the ternary complex with GSH. The crystal structure of this inactivated assembly provides first insight into the binding interactions between an antivitamin B_{12} and CblC, as well as into the organization of GSH and a base-off cobalamin in the active site of this enzyme.*

Vitamin B_{12} (cyanocobalamin, CNCbl) and other cobalamins (Cbls) are indispensable for the mammalian metabolism[1] on account of the essential cofactor activities of coenzyme B_{12} (AdoCbl) and methylcobalamin (MeCbl).[2] To provide mammalian cells with AdoCbl and MeCbl, natural Cbls are first transformed into cob(II)alamin (Cbl^{II}) by the Cbl-processing chaperone CblC (also named MMACHC, for methylmalonic aciduria type C and homocystinuria).[3] CblC binds Cbls base-off and removes their axial Co_β ligand[3c,4] to furnish Cbl^{II}, the relevant biosynthetic precursor of AdoCbl and MeCbl.[3c] Cbls that are transported into cells, but are not deligated there by CblC, remain metabolically inert and have been classified as B_{12} antivitamins.[5] Such inert vitamin B_{12} derivatives induce symptoms of B_{12} deficiency in laboratory animals,[6] as does a dysfunctional CblC in humans.[3b]

To clarify still puzzling roles of Cbls in humans,[1,7] B_{12} deficiency is studied in laboratory animals. The application of B_{12} antivitamins[5,8] is a rather animal-friendly means in such studies.[6,9] Indeed, the antivitamin B_{12} 4-ethylphenylcobalamin (**1**, EtPhCbl) induced functional B_{12} deficiency in mice.[6,10] Unfortunately, **1** is susceptible to light-induced cleavage of its Co–C bond, which uncages its locked B_{12} activity.[10] Herein, we report the preparation of 2-(2,4-difluorophenyl)ethynylcobalamin (**3**, F2PhEtyCbl; Figure 1), an analogue of the earlier studied light-stable 2-phenylethynylcobalamin (**2**, PhEtyCbl), which was made more resistant towards hydrolysis by two fluorine substituents.[11,12] We also investigated the interactions of **2** and **3** with the human B_{12}-processing enzyme CblC, and describe the crystal structure of the ternary complex of CblC with glutathione (GSH) and **3**, providing unprecedented insight into a holo-CblC complex that is rendered inactive by an antivitamin B_{12}.

F2PhEtyCbl (**3**) was prepared in 58% yield by reduction of aquocob(III)alamin (H_2OCbl) with triethylammonium formate in the presence of 2-(2,4-difluorophenyl)ethynyl iodide, a method developed for the synthesis of PhEtyCbl (**2**).[11a] The reaction probably follows a radical process initiated by in situ generated Cbl^{II}, as proposed for the synthesis of **2**.[11a] The UV/Vis spectrum of **3** (Figure 2) is similar to that of PhEtyCbl (**2**),[11] but differs significantly from the spectra of the organometallic B_{12} cofactors AdoCbl and MeCbl.[13] In neutral aqueous solution, F2PhEtyCbl (**3**) exists in the base-on form, and a strong acid is needed to

[*] Dr. M. Ruetz, Dr. R. Salchner, M. Sc. C. Kieninger, Prof. B. Kräutler
Institute of Organic Chemistry and Center for Molecular Biosciences
University of Innsbruck, 6020 Innsbruck (Austria)
E-mail: bernhard.kraeutler@uibk.ac.at
Dr. M. Ruetz, Dr. C. Gherasim, Prof. R. Banerjee
University of Michigan Medical School
Ann Arbor (USA)
E-mail: rbanerjee@umich.edu
A. Shanmuganathan, A. Karasik, Prof. M. Koutmos
Department of Biochemistry
Uniformed Services University of the Health Sciences
Bethesda (USA)
E-mail: markos.koutmos@usuhs.edu
Dr. K. Wurst
Institute of General, Inorganic and Theoretical Chemistry
University of Innsbruck (Austria)
Dr. R. Salchner
Current address: Watercryst GmbH & Co
Kematen (Austria)
Dr. C. Gherasim
Current address: Department of Pathology
University of Utah School of Medicine
Salt Lake City, UT (USA)
Supporting information and the ORCID identification number(s) for the author(s) of this article can be found under: https://doi.org/10.1002/anie.201701583.

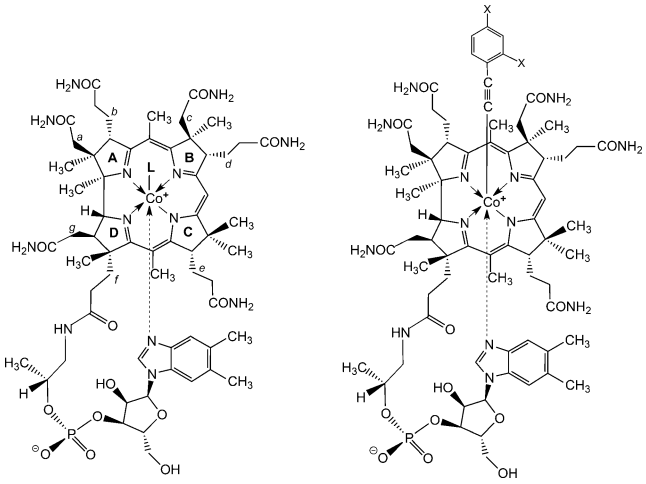

Figure 1. Left: General structural formula of important Cbls: vitamin B_{12} (L = CN, cyanocob(III)alamin, CNCbl), coenzyme B_{12} (L = 5′-adenosyl: 5′-deoxyadenosylcob(III)alamin, AdoCbl), methylcob(III)alamin (L = methyl: MeCbl), cob(II)alamin (L = e^-: Cbl^{II}), 4-ethylphenylcob(III)alamin (**1**; L = 4-ethylphenyl: EtPhCbl), and aquocob(III)alamin (L = H_2O^+: H_2OCbl). Right: Structural formula of 2-phenylethynylcobalamin (**2**, PhEtyCbl, X = H) and 2-(2,4-difluorophenyl)ethynylcobalamin (**3**, F2PhEtyCbl, X = F).

remove the 5,6-dimethylbenzimidazole (DMB) base by protonation to give **3-H**$^+$. The formation of base-off **3-H**$^+$ is accompanied by characteristic hypsochromic shifts of the UV/Vis absorption maxima (Figure 2). A pK_a value of 0.75 was determined for **3-H**$^+$ (see the Supporting Information, Figure S11), which corresponds to a [base-on]/[base-off] equilibrium of about 10^5 for **3**, indicative of strong stabilization of the base-on form.

The molecular formula and the basic structure of F2PhEtyCbl (**3**) were delineated from a MALDI-TOF mass spectrum, an IR spectrum (band of the C≡C bond at $\tilde{\nu}$ = 2130.5 cm^{-1}; see Figure S2) and detailed ^{1}H NMR and ^{13}C NMR studies of a solution of **3** in CD_3OD (Figure S3). Orthorhombic crystals of **3** (space group $P2_12_12_1$) were grown from aqueous acetone. The crystal structure of **3** shows a base-on Cbl with the 2,4-difluorophenylethynyl ligand at the top (Figures 2, S5, and S6 and Table S1). The geometries and bond lengths of the inner coordination spheres of the cobalt centers of **3** and PhEtyCbl (**2**)[11] are similar. As in **2**[11] and in CNCbl,[14,15] the axial bonds of **3** are short (Co–C1L 1.877(7) Å, Co–N3N 2.071(5) Å). Likewise, the ethynyl group of **3** exhibits a short (1.206(9) Å) and nearly linear C1L≡C2L triple bond, with Co-C1L-C2L and C1L-C2L-CL3 bond angles of 170.5(5)° and 176.1(7)°, respectively. The plane of the 2,4-difluorophenyl group is nearly parallel to that of the DMB base, twisted by only 23.1(3)°.

When a solution of F2PhEtyCbl (**3**) in DMSO was heated to 100 °C for 24 h, UV/Vis spectroscopy and HPLC analysis (Figure S7) indicated complete retention of the Co–C bond. As reported earlier for ethynyl-Cbl[14] and **2**,[11,12] solutions of **3** were stable in sunlight (Figure S8). In aqueous solution, **3** underwent slow pH-dependent hydrolysis to H_2OCbl. At pH 2, **3** hydrolyzed with pseudo-first-order kinetics and with a half-life of about 20 h at room temperature. The roughly

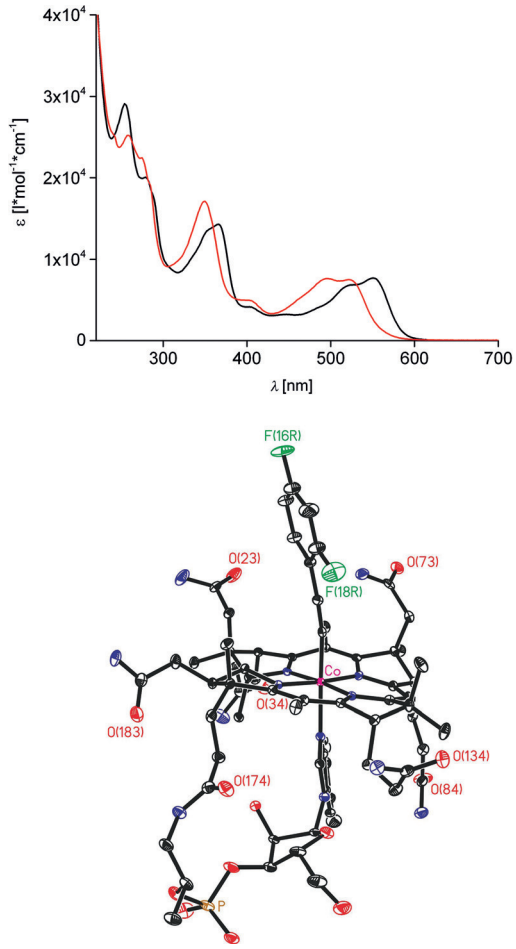

Figure 2. Top: UV/Vis spectra of an aqueous solution of F2PhEtyCbl (**3**, c = 55 μM) in H_2O (black trace) and immediately after acidification with $HClO_4$ (to 1 M) to give base-off H-F2PhEtyCbl$^+$ (**3-H**$^+$, red trace). Bottom: Model of the crystal structure of **3**. N blue, O red, P orange, Co pink, F green. See the Supporting Information for details and a model of **3** in stereoprojection. Thermal ellipsoids set at 30% probability.

first-order dependence on the H_3O^+ concentration from pH 0 to pH 4 (Figures S9 and S10) allowed the hydrolysis-based half-life of **3** at pH 7 to be estimated as about 10^7 h. Hence, **3** can be considered as being stable under physiological conditions.

The binding of F2PhEtyCbl (**3**) or PhEtyCbl (**2**) to CblC was accompanied by blue shifts of the UV/Vis absorptions, as observed with MeCbl[16] and EtPhCbl.[10] The conversion of base-on **3** (or **2**) into the corresponding base-off form was slow, as revealed by the UV/Vis spectroscopic changes upon binding (Figures 3 and S12). Addition of the cosubstrate glutathione (GSH) caused further hypsochromic shifts of the maxima. In the presence of GSH, the binding of **3** (or **2**) to CblC was accompanied by a complete switch to the base-off form, suggesting that GSH binding plays a structuring role in holo-CblC (Figures 3 and S13). Accommodation of the large organometallic moiety of **3** in CblC was consistent with expectations based on the crystal structure of CblC with bound MeCbl.[17] Isothermal calorimetry (ITC) revealed a high binding affinity of alkynyl-Cbl **3** to human CblC

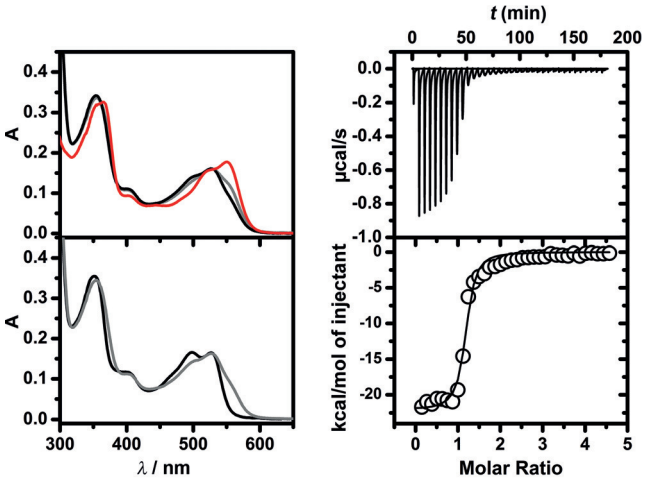

Figure 3. Biochemical studies with CblC, F2PhEtyCbl (**3**), and GSH. Top left: Time-dependent UV/Vis spectra for the binding of **3** to CblC. The original spectrum of **3** is shown in red, the final spectrum after 60 min in black. Bottom left: Spectral changes upon subsequent binding of GSH. The initial and final spectra are shown in gray and black, respectively. Right: ITC data for a representative titration of CblC with **3** in the presence of GSH (10 μM CblC, 200 μM **3**, 1 mM GSH). The binding isotherm (lower panel) was fitted to a model with one binding site (see the Supporting Information for details).

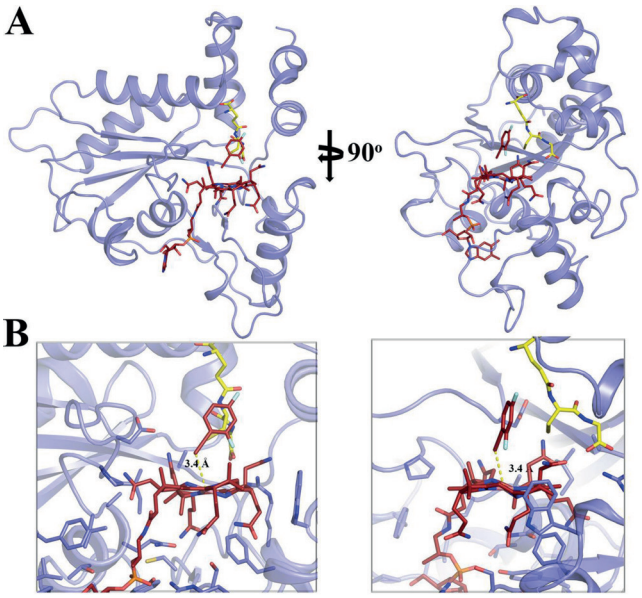

Figure 4. A) Two views of the structure of GSH and F2PhEtyCbl (**3**) bound to CblC (light blue) shown as a cartoon. GSH (yellow) and **3** (dark red) ligands are shown as sticks. B) Two corresponding close-up views of this ternary complex.

($K_D = 129 \pm 13$ nM) in the presence of GSH, which is about four times lower than that for **2** ($K_D = 30 \pm 5.6$ nM; Figures 3 and S15). Incubation of 17–20 μM solutions of **2** or **3** and 10 mM of GSH together with 50 μM CblC at 20 °C for 12 h did not lead to detectable degradation of either alkynyl-Cbl (Figure S14). Hence, in contrast to MeCbl, which is rapidly demethylated by CblC and GSH ($k_{obs} = 0.6\ min^{-1}$),[10] **2** and **3** were not modified by this universal B_{12} "tinkerer" ($k_{obs} < 3 \times 10^{-7}\ s^{-1}$).

The stable ternary complex of alkynyl-Cbl **3**, GSH, and CblC was crystallized by the vapor diffusion method. Crystals grew in the $P6_122$ space group with one monomer in the asymmetric unit (Table S2). The structure was solved to 2.5 Å resolution (Figures 4 and S16) by molecular replacement by using a previous structure of CblC as a search model (PDB No. 3SC0),[17] but omitting the MeCbl cofactor, loops, and areas with high B-factors. Clear electron density could be assigned to the Cbl and GSH ligands, which were then modeled and subsequently refined. Antivitamin **3** was bound in a base-off form. In this structure (with **3** and GSH bound to CblC) and in the one with MeCbl bound to CblC,[17] the position and interactions of the DMB base were not distinguishable. Likewise, the *a* and *g* acetamide side chains at rings A and D, as well as the *b* propionamide, are tightly hydrogen-bonded to the protein part and are found in identical positions in both crystal structures. Among the distinct differences, the *d* and *e* propionamide and the *c* acetamide side chains at rings B and C adopt unique arrangements in the structure of CblC bound to F2PhEtyCbl and GSH (Figures 4 and 5). However, they are not as close to each other and to the Co atom (with Co···N45, Co···N52, and N45···N52 distances of 4.2, 5.1, and 4.3 Å, respectively), as in MeCbl bound to CblC,[17] thus providing better access to the

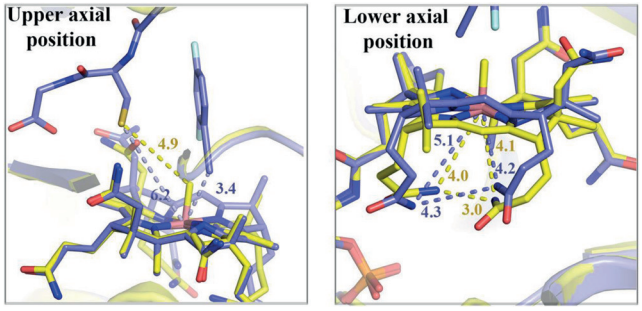

Figure 5. Structural comparison of CblC with bound MeCbl (yellow) and the ternary complex of CblC with GSH and F2PhEtyCbl (blue). On the left, the environment of the upper axial Co position in the vicinity of the GSH ligand is presented. On the right, the environment of the lower axial Co position is shown. Blue and yellow dotted lines represent selected distances in the GSH- and F2PhEtyCbl-bound and MeCbl-bound CblC structures, respectively. Note the arrangement of the "tucked-in" *d* and *e* propionamide side chains.

lower axial position. In MeCbl bound to CblC, the *d* and *e* propionamide side chains approach each other, and the Co center is even closer (with Co···N45, Co···N52, and N45···N52 distances of 4.1, 4.0, and 3.0 Å, respectively). Such striking "tucked-in" structures appear to be a hallmark of Cbls bound to CblC[17,18] that is crucial for activation of the bound corrin for conversion by reductive dealkylation.[3c,4] Remarkably, in the CblC ternary complex with GSH, the hydrogen-bonding network between the corrin ring of **3** and its surrounding protein milieu is largely similar to that of the binary complexes of CblC with MeCbl[17] and AdoCbl.[18]

Distinct electron density was observed in the vicinity of the Co atom where a β-axial ligand would be expected (Figure S17). However, we could not discern an ethynyl

carbon atom directly bound to the Co center from the electron density clearly associated with the F2PhEty group. Based on a calculated unbiased composite omit map, the 2,4-difluorophenyl ring was observed in a different position compared to the free form of F2PhEtyCbl (**3**) and farther away from the cobalt atom (Figure 4). The planes of the phenyl rings in free **3** and in its CblC-bound form were roughly perpendicular with respect to each other. Moreover, the axis of the aromatic ring no longer pointed to a Co d_{z^2} orbital. Hence, the 2,4-difluorophenylethynyl group, as it best fits the experimental electron density, is too far away from the Co center to be coordinated to it. This model gives a distance of 3.4 Å between the Co^{II} center of Cbl and C1L of the F2PhEty fragment (see Figure 4). Therefore, we posit that the intense synchrotron radiation used during data collection has led to cleavage of the Co–C bond, possibly in a reductive process,[18–20] furnishing (base-off) Cbl^{II} and a weakly bound F2PhEty anion.

The electron density clearly correlating with GSH allowed for a first characterization of its protein environment in CblC and its location with respect to the bound Cbl (Figures 6A and S18). An extended network of protein–GSH interactions anchored this ligand to its binding pocket, namely a combination of 1) multiple hydrogen-bond interactions with all three peptide moieties (Glu, Cys, Gly) of GSH and 2) hydrophobic stacking interactions between the glycine moiety and protein residues (F223, Y224, and A159). Most of the GSH ligand is enclosed by the protein and the bound Cbl, with 70% of the total GSH surface area covered by the protein and 20% covered by Cbl. In fact, the weakly bound F2PhEty group packs tightly against GSH, and S_{GSH} is near the aromatic ring of the F2PhEty fragment, with distances varying from 4.2 to 5.1 Å. However, the neighboring CH_2 group of GSH is found at distances of 3.9 to 4.0 Å from the F2PhEty ring, which is indicative of CH–π contacts. In contrast, in a model of the protein with bound intact **3**, steric clashes with the GSH ligand occur (Figures S19 and S20).

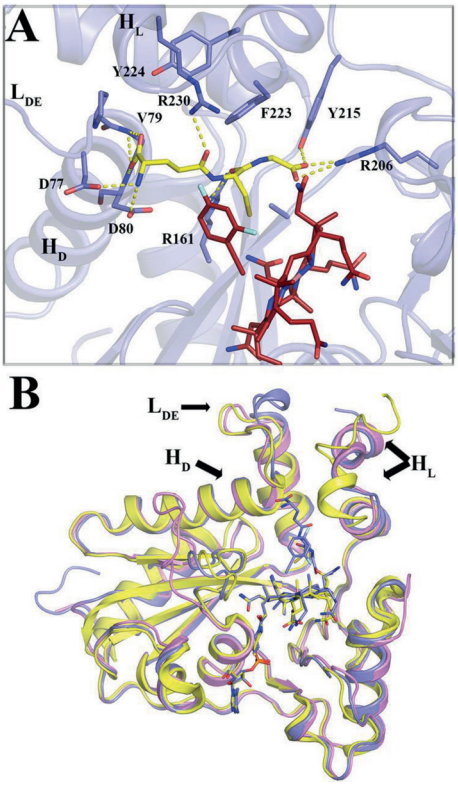

Figure 6. A) The GSH-binding environment in the ternary complex with CblC and F2PhEtyCbl (**3**). GSH and **3** are shown as yellow and dark red sticks, respectively. Protein residues of the GSH binding pocket are shown as blue sticks, and hydrogen bonds are represented by yellow dotted lines. B) Structural superposition of apo (pink), MeCbl-bound (yellow), and GSH- and F2PhEtyCbl-bound CblC (blue). MeCbl (yellow), GSH (blue), and F2PhEtyCbl (blue) ligands are displayed as sticks. The three major structural differences are highlighted with arrows.

Previous reports based on available structures, sequence conservation, and biochemical analysis[17,18,21] suggested and identified R230, R161, and R206 as putative residues that are important for GSH binding. Indeed, our structure determination confirmed the crucial role of these three arginine residues and identified R161 as the anchor of GSH in the CblC active site through interactions of its guanidinium group and the carboxamide group of the cysteine moiety of GSH. However, Y215, D77, and D80 were now additionally shown to form hydrogen bonds to GSH, pointing to an induced fit by the protein that had previously not been predicted. The sulfur center (S_{GSH}) of GSH, key to the Cbl dealkylation activity of CblC, is situated in the vicinity of the bound Cbl with a Co–S_{GSH} distance of 6.3 Å. This corresponds to a calculated distance of 4.9 Å between the methyl carbon atom in a superimposed CblC-bound MeCbl and S_{GSH} in our structure. This positioning of S_{GSH} relative the bound corrin does not fulfill the geometric constraints of the proposed S_N2-type mechanism of the dealkylation by GSH. Strikingly, the S_{GSH} group also lacks any close contacts that would facilitate its deprotonation and increase its nucleophilicity.

The protein fold of the inactive ternary CblC complex studied herein reveals distinct differences when compared to the previously described structures of apo-CblC (PDB No. 3SBZ) and MeCbl-bound CblC (MeCbl:CblC, PDB No. 3SC0;[17] Figure 6). The LDE loop is found in a unique arrangement as a result of the binding of GSH in the ternary complex. To accommodate its glutamate moiety, the cosubstrate GSH also promotes a rearrangement of the N-terminal moiety of the LDE loop, as the well as the C-terminal region of the preceding helix (HD), including residues 77–80. Moreover, the terminal helix (HL) in the four-helix cap region adopts different conformations in the CblC structures with MeCbl or F2PhEtyCbl (**3**) bound. However, the HL helix appears in the same conformation in both the apo- and F2PhEtyCbl-bound CblC structures, hinting at the dynamic nature of this helix.

The base-off forms of **2** and **3** bound effectively to CblC in the presence of glutathione (GSH). However, as also shown here, inactive ternary complexes were thus obtained that were incapable of generating Cbl^{II}. The lack of reactivity of the antivitamin B_{12} **3** was employed to trap the cosubstrate GSH in a previously unattainable form of the ternary complex, providing the first crystal structure of holo-CblC with GSH and an antivitamin B_{12} bound at the same time. This study

pinpointed the specific protein and Cbl contributions in anchoring GSH, providing a rational structural basis for future work with mutant proteins. For example, two severe pathogenic mutations of CblC (R161G and R161Q) can now be rationalized, based on the key role of R161 in binding GSH. B_{12} antivitamins that are more resistant towards X-ray reduction than **3** in the complex with GSH may help define the structural basis for the dealkylation activity of CblC more precisely.

As explored here for a B_{12}-processing enzyme, B_{12} antivitamins producing inactive enzyme complexes may be helpful for solving their crystal structures. Future studies are also required to learn more about the applicability of B_{12} antivitamins, such as **3**. In fact, EtPhCbl (**1**) not only induced "functional B_{12} deficiency" in mice,[6] but also helped in eradicating resistant Gram-negative human pathogens.[22] Studies of B_{12} antivitamins and related Cbls as anticancer agents have also raised interest.[5,8,23] Indeed, **3** is a promising, light-stable alternative to the antivitamin B_{12} **1**,[6,10] and might also be a very versatile biomedical tool. Long-term experiments with animals in close to natural habitats[6] may be feasible with **3**, and will specifically help in expanding our knowledge of the physiological effects of B_{12} deficiency, and in reducing the gap in understanding its downstream pathophysiological effects in humans.

Experimental Section

See the Supporting Information for materials, instruments, synthetic procedures, spectral characterization of compounds and enzyme complexes, biochemical studies, and X-ray crystallography.

CCDC 1530214 (F2PhEtyCbl, **3**) contains the supplementary crystallographic data for this paper. These data can be obtained free of charge from The Cambridge Crystallographic Data Centre. Coordinates and structure factors for F2PhEtyCbl:GSH:CblC have been deposited in the Protein Data Bank as entry 5UOS.

Acknowledgements

We are grateful to the Austrian Science Foundation (FWF) for support of the research in Innsbruck (current project: FWF P-28892). We also thank the National Institute of General Medical Sciences and the National Cancer Institute Collaborative Access Team (GM/CA CAT) at the Advanced Light Source for beam time. This work was supported in part by the American Heart Association (13SDG14560056, to M.K.) and the National Institute of Health (NIH, grant DK45776, to R.B.).

Conflict of interest

The authors declare no conflict of interest.

Keywords: antivitamins · enzyme inhibitors · glutathione · protein crystallography · vitamin B_{12}

How to cite: *Angew. Chem. Int. Ed.* **2017**, *56*, 7387–7392
Angew. Chem. **2017**, *129*, 7493–7498

[1] R. Carmel, R. Green, D. S. Rosenblatt, D. Watkins, *Hematology Am. Soc. Hematol. Educ. Program* **2003**, 62–81.
[2] a) *Vitamin B_{12} and B_{12} Proteins* (Eds.: B. Kräutler, D. Arigoni, B. T. Golding), Wiley-VCH, Weinheim, **1998**; b) *Chemistry and Biochemistry of B_{12}* (Ed.: R. Banerjee), Wiley, New York, **1999**; c) R. Banerjee, S. W. Ragsdale, *Annu. Rev. Biochem.* **2003**, *72*, 209–247; d) R. G. Matthews, M. Koutmos, S. Datta, *Curr. Opin. Struct. Biol.* **2008**, *18*, 658–666.
[3] a) J. P. Lerner-Ellis, J. C. Tirone, P. D. Pawelek, C. Dore, J. L. Atkinson, D. Watkins, C. F. Morel, T. M. Fujiwara, E. Moras, A. R. Hosack, G. V. Dunbar, H. Antonicka, V. Forgetta, C. M. Dobson, D. Leclerc, R. A. Gravel, E. A. Shoubridge, J. W. Coulton, P. Lepage, J. M. Rommens, K. Morgan, D. S. Rosenblatt, *Nat. Genet.* **2006**, *38*, 93–100; b) L. Hannibal, P. M. DiBello, M. Yu, A. Miller, S. H. Wang, B. Willard, D. S. Rosenblatt, D. W. Jacobsen, *Mol. Genet. Metab.* **2011**, *103*, 226–239; c) R. Banerjee, C. Gherasim, D. Padovani, *Curr. Opin. Chem. Biol.* **2009**, *13*, 484–491.
[4] L. Hannibal, J. Kim, N. E. Brasch, S. H. Wang, D. S. Rosenblatt, R. Banerjee, D. W. Jacobsen, *Mol. Genet. Metab.* **2009**, *97*, 260–266.
[5] B. Kräutler, *Chem. Eur. J.* **2015**, *21*, 11280–11287.
[6] E. Mutti, M. Ruetz, H. Birn, B. Kräutler, E. Nexo, *Plos One* **2013**, *8*, e75312.
[7] a) G. Scalabrino, *Prog. Neurobiol.* **2009**, *88*, 203–220; b) E. V. Quadros, *Br. J. Haematol.* **2010**, *148*, 195–204; c) L. R. Solomon, *Blood Rev.* **2007**, *21*, 113–130; d) M. A. Moreno-Garcia, D. S. Rosenblatt, L. A. Jerome-Majewska, *Nutrients* **2013**, *5*, 3531–3550.
[8] F. Zelder, M. Sonnay, L. Prieto, *ChemBioChem* **2015**, *16*, 1264–1278.
[9] G. Scalabrino, M. Peracchi, *Trends Mol. Med.* **2006**, *12*, 247–254.
[10] M. Ruetz, C. Gherasim, S. N. Fedosov, K. Gruber, R. Banerjee, B. Kräutler, *Angew. Chem. Int. Ed.* **2013**, *52*, 2606–2610; *Angew. Chem.* **2013**, *125*, 2668–2672.
[11] a) M. Ruetz, R. Salchner, K. Wurst, S. Fedosov, B. Kräutler, *Angew. Chem. Int. Ed.* **2013**, *52*, 11406–11409; *Angew. Chem.* **2013**, *125*, 11617–11620; b) M. Chromiński, A. Lewalska, D. Gryko, *Chem. Commun.* **2013**, *49*, 11406–11408.
[12] N. A. Miller, T. E. Wiley, K. G. Spears, M. Ruetz, C. Kieninger, B. Kräutler, R. J. Sension, *J. Am. Chem. Soc.* **2016**, *138*, 14250–14256.
[13] C. Giannotti in *B_{12}, Vol. I* (Ed.: D. Dolphin), Wiley, New York, **1982**, pp. 393–430.
[14] J. M. Pratt, *Inorganic Chemistry of Vitamin B_{12}*, Academic Press, New York, **1972**.
[15] L. Randaccio, S. Geremia, G. Nardin, J. Würges, *Coord. Chem. Rev.* **2006**, *250*, 1332–1350.
[16] J. Kim, L. Hannibal, C. Gherasim, D. W. Jacobsen, R. Banerjee, *J. Biol. Chem.* **2009**, *284*, 33418–33424.
[17] M. Koutmos, C. Gherasim, J. L. Smith, R. Banerjee, *J. Biol. Chem.* **2011**, *286*, 29780–29787.
[18] D. S. Froese, T. Krojer, X. C. Wu, R. Shrestha, W. Kiyani, F. von Delft, R. A. Gravel, U. Oppermann, W. W. Yue, *Biochemistry* **2012**, *51*, 5083–5090.
[19] a) K. Gruber, R. Reitzer, C. Kratky, *Angew. Chem. Int. Ed.* **2001**, *40*, 3377–3380; *Angew. Chem.* **2001**, *113*, 3481–3484; b) L. Randaccio, S. Geremia, J. Würges, *J. Organomet. Chem.* **2007**, *692*, 1198–1215.
[20] D. Lexa, J. M. Savéant, *Acc. Chem. Res.* **1983**, *16*, 235–243.
[21] a) C. Gherasim, M. Ruetz, Z. Li, S. Hudolin, R. Banerjee, *J. Biol. Chem.* **2015**, *290*, 11393–11402; b) J. P. Lerner-Ellis, N. Anastasio, J. H. Liu, D. Coelho, T. Suormala, M. Stucki, A. D. Loewy, S. Gurd, E. Grundberg, C. F. Morel, D. Watkins, M. R. Baumgartner, T. Pastinen, D. S. Rosenblatt, B. Fowler, *Hum. Mutat.* **2009**, *30*, 1072–1081.

[22] M. B. Guzzo, H. T. Nguyen, T. H. Pham, M. Wyszczelska-Rokiel, H. Jakubowski, K. A. Wolff, S. Ogwang, J. L. Timpona, S. Gogula, M. R. Jacobs, M. Ruetz, B. Kräutler, D. W. Jacobsen, G. F. Zhang, L. Nguyen, *Plos Pathog.* **2016**, *12*, e1005949.
[23] a) F. Zelder, R. Alberto in *Handbook of Porphyrin Science*, *Vol. 25* (Eds.: K. M. Kadish, K. M. Smith, R. Guilard), World Scientific, Singapore, **2012**, pp. 84–132; b) J. Rossier, D. Hauser, E. Kottelat, B. Rothen-Rutishauser, F. Zobi, *Dalton Trans.* **2017**, *46*, 2159–2164.

Manuscript received: February 21, 2017
Version of record online: May 23, 2017

